HAL
open science

Multibody kinematics optimization with marker projection improves the accuracy of the humerus rotational kinematics

Mickaël Begon, Colombe Belaise, Alexandre Naaim, Arne Lundberg, Laurence Cheze

To cite this version:

Mickaël Begon, Colombe Belaise, Alexandre Naaim, Arne Lundberg, Laurence Cheze. Multibody kinematics optimization with marker projection improves the accuracy of the humerus rotational kinematics. Journal of Biomechanics, 2017, 62, pp.117-123. 10.1016/j.jbiomech.2016.09.046 . hal-01635717

HAL Id: hal-01635717

https://hal.science/hal-01635717

Submitted on 15 Nov 2017

HAL is a multi-disciplinary open access archive for the deposit and dissemination of scientific research documents, whether they are published or not. The documents may come from teaching and research institutions in France or abroad, or from public or private research centers.

L'archive ouverte pluridisciplinaire **HAL**, est destinée au dépôt et à la diffusion de documents scientifiques de niveau recherche, publiés ou non, émanant des établissements d'enseignement et de recherche français ou étrangers, des laboratoires publics ou privés.

Multibody kinematic optimization with marker projection improves the accuracy of the humerus rotational kinematics

Mickaël Begon[a], Colombe Bélaise[a], Alexandre Naaim[b], Arne Lundberg[d], Laurence Chèze[c]

[a] *Department of Kinesiology, Université de Montréal, H3C 3J7, Montreal, QC, CANADA*
[b] *CIC INSERM 1432, Plateforme d'Investigation Technologique, CHU Dijon, FRANCE*
[c] *Univ Lyon, Université Lyon 1, IFSTTAR, LBMC UMR_T9406, F69622, Lyon, FRANCE*
[d] *Karolinska Institutet, Stockholm, SWEDEN*

Corresponding author

Mickaël Begon

Department of Kinesiology, Université de Montréal

Sainte-Justine Hospital Research Center

Address: CEPSUM – 2100, boul. Édouard-Montpetit Bureau 8202

C.P. 6128, succursale Centre-ville

Montréal (Québec) H3C 3J7 CANADA

Phone: 514 343-6151; Fax: 514 343-2181

mickael.begon@umontreal.ca

Original Article

Word count: 3578

Abstract

Markers put on the arm undergo large soft tissue artefact (STA). Using markers on the forearm, multibody kinematic optimisation (MKO) helps improve the accuracy of the arm kinematics especially its longitudinal rotation. However deleterious effect of STA may persist and affect other segment estimate. The objective was to present an innovative multibody kinematic optimization algorithm with projection of markers onto a requested axis of the local system of coordinates, to cancel their deleterious effect on this degree-of-freedom. Four subjects equipped with markers put on intracortical pins inserted into the humerus, on skin (scapula, arm and forearm) and subsequently on rigid cuffs (arm and forearm) performed analytic, daily-living, sports and range-of-motion tasks. Scapulohumeral kinematics was estimated using 1) pin markers (reference), 2) single-body optimisation, 3) MKO, 4) MKO with projection of all arm markers and 5) MKO with projection of a selection of arm markers. Approaches 2-4 were applied to markers put on the skin and the cuff. The main findings were that multibody kinematic optimization improved the accuracy of 40 to 50% and the projection algorithm added an extra 20% when applied to cuff markers or a selection of skin markers (all but the medial epicondyle). Therefore, the projection algorithm performed better than multibody and single-body optimizations, especially when using markers put on a cuff. Error of humerus orientation was reduced by half to finally be less than 5°. In conclusion, this innovative algorithm is a promising approach for estimating accurate upper-limb kinematics.

Keywords

Upper-limb; Multibody kinematic optimization; Marker projection algorithm.

1. Introduction

An accurate estimate of the three-dimensional scapulohumeral joint kinematics – especially axial rotation and elevation – can be clinically relevant to assess the rotator cuff muscles disorders (Anglin and Wyss, 2000; Lawrence et al., 2014). Unfortunately, sensors or markers put on the arm undergo soft tissue artefact (STA) (Blache et al., 2016; Hamming et al., 2012) that compromises the accuracy. In particular, the axial rotation tends to be underestimated (Cutti et al., 2005a; Ludewig et al., 2002; Schmidt et al., 1999) and errors up to 30° on the arm axial rotation were found due to STA, when using an electromagnetic sensor attached to the lateral aspect of the arm (Hamming et al., 2012). Using seven skin markers spread over the arm, this error can be reduced by about 10° (Begon et al., 2015). However, this last study has shown that single-body optimization with marker weightings fails to improve the arm kinematics, since optimal weightings are subject- and task-specific (Begon et al., 2015). According to the marker-cluster geometrical transformations proposed by Dumas et al. (2014) to describe STA, the movement of a cluster of markers put on the arm with respect to the bone corresponds mainly to a rigid transformation (*i.e.* translation and rotation) (Blache et al., 2016). Consequently, algorithms using additional markers/sensors on the forearm have been the most promising avenue to accurately estimate the scapulohumeral joint kinematics (Cutti et al., 2005b; Lin and Karduna, 2013; Roux et al., 2002; Schmidt et al., 1999). In fact, there is less soft tissue around the forearm and the humeroulnar joint can be modelled as one degree-of-freedom (DoF) in flexion, which decreases the complexity of the multibody system. However, these models have not been validated using the true humeral bone kinematics for a large variety of movements yet, and some algorithms fail when the elbow is fully extended.

In multibody kinematic optimization, markers put on the forearm may correct the arm axial rotation (Roux et al., 2002). Markers put on the olecranon and proximally on the dorsal border of the ulna also may improve the estimation of the arm axial rotation because of the small soft tissue thickness and, above all, because some markers are distant from the arm longitudinal axis when the elbow is bent. The drawback of multibody least-squares minimization is that markers with large STA may negatively affect the kinematics of adjacent segments. For example, some markers on the arm may affect the forearm pro-supination estimation. To the best of our knowledge, no algorithm has been proposed to cancel this deleterious effect. To address this shortcoming, said STA-affected markers could be projected onto an axis of the local frame to ensure that they do not participate to the estimation of the rotation along this axis.

The performance of multibody kinematic optimization algorithms depends on the joint constraints (Duprey et al., 2010), model parameters (e.g. segment length (El Habachi et al., 2013)) and the markers/sensors involved (Begon et al., 2008). Unfortunately, no optimal marker set or sensor placement exist yet (Anglin and Wyss, 2000). Electromagnetic sensors and cuffs with reflective markers remain the standard in upper-limb biomechanics (Anglin and Wyss, 2000). Also, it has been recommended to not attach markers/sensors on anatomical landmarks (Kontaxis et al., 2009). However, recent studies have highlighted that the medial epicondyle presented small STA (Blache et al., 2016) and skin markers performed well (Begon et al., 2015), by comparison with a single electromagnetic sensor (Hamming et al., 2012). Our hypothesis was that skin markers undergo different STA that compensate each other, but this was not confirmed. Since seven markers were put on the arm, it was expected that, in line with simulation-based studies (Challis, 1995; Monnet et al., 2010), the accuracy achieved from them outperformed that

from a single 6-DoF sensor. New multibody kinematic optimization algorithms should then be assessed using different marker sets.

The objective of this study was to present an innovative multibody kinematic optimization algorithm, based on the projection of all or selected markers, onto a requested axis of the local system of coordinates (SoC), to cancel their deleterious effect on this DoF. Its benefit was assessed on the upper-limb against true bone kinematics, by comparison to single-body and standard multibody optimizations.

2. Methods

2.1. Experiment

The experimental protocol with pin insertion and skin markers is described in Dal Maso et al. (2015) and Begon et al. (2015). It was approved by the local ethic committees of the Université de Montréal and Karolinska Institutet. Four asymptomatic males (ages: 41, 32, 44 and 27 years, heights: 1.82, 1.72, 1.77 and 1.65 m, masses: 80, 82, 115 and 57 kg) volunteered in this study. Markers were placed on a pin screwed into their humerus and on skin. Subsequently, markers placed on thermoformed cuffs attached to the arm and forearm replaced the skin markers. Marker trajectories were acquired at 300 Hz using an 18-camera motion analysis system (Oxford Metrics Ltd., Oxford, UK). **Fig. 1** illustrates the markers needed for this secondary use of data. Participants performed 18 movements allocated in four categories (**Tab. 1**): 1) analytic movements similar to Hamming et al. (2012); 2) mimics of activities of daily living (ADL) (van Andel et al., 2008); 3) mimics of sports activities and 4) movements with maximal range of motion (Haering et al., 2014). In the condition with cuffs, only analytic movements and ADL were performed due to the anesthetic duration.

Please insert Fig. 1 here

Please insert Fig. 2 here

Please insert Tab. 1 here

2.2. Models and kinematic reconstruction

For each participant, five multibody kinematic models were developed according to the framework of Kontaxis et al. (2009) and the ISG recommendations (Wu et al., 2005) about anatomical frames definition. They mainly differed in joint and motor constraints. Partially described in Jackson et al. (2012), the models were composed of a common root: thorax

(6 DoFs), clavicle (2 DoFs), scapula (3 DoFs) (**Fig. 1**). Skin markers were used for these three body segments as proposed by Jackson et al. (2012), including three markers put on the acromion. The joint between the pelvis and thorax was functionally located (Ehrig et al., 2006), while sternoclavicular and acromioclavicular joint locations were defined using markers placed on the most ventral point on the sternoclavicular joint and the most dorsal point on the acromioclavicular joint (Michaud et al., 2016). The generalized coordinates (**q**) of this common root were first obtained by solving a non-linear least-squares problem as described by Laitenberger et al. (2015).

In the 1st and 2nd models (termed as *Humerus* and *Arm* models, respectively), the arm had 6 DoFs with respect to the scapula; the two models differed in the markers used in the inverse kinematics algorithm: pin markers vs. skin/cuff markers, respectively. The *Humerus* model corresponded to the reference bone kinematics. The *Arm* model was about making a single-body optimization. The 3rd to 5th models (*UpLimb, UpLimbP* and *UpLimbS*) included the arm (3 DoFs) and forearm (1 DoF) with skin markers. *UpLimb* model corresponded a standard multibody kinematic optimisation. In the *UpLimbP* model, all the skin markers of the arm were projected onto its longitudinal axis (*y*). In the *UpLimbS* model, selected skin markers (all of the arm but the medial epicondyle) were projected onto its longitudinal axis. The coordinate systems of the segments and joints were in accordance with the ISG recommendations, based on the same anatomical landmarks for all the models. As suggested by Michaud et al. (2016), the scapulohumeral joint center was determined using the predictive method of Rab et al. (2002). The humeroulnar joint was functionally located (O'Brien et al., 1999).

In all the models, the generalized coordinates (**q**) of the upper-limb were obtained by solving a non-linear least-squares problem and adapted to include a projection function of observed marker global coordinates $\mathbf{M}_{obs}^{G}$ onto desired axes, $\mathbf{P}_{obs}^{G} = p(\mathbf{M}_{obs}^{G}, \mathbf{q})$:

$$\min_{\mathbf{q}} \frac{1}{2} \left\| p(\mathbf{M}_{obs}^{G}, \mathbf{q}) - f(\mathbf{q}) \right\|^2, \tag{1}$$

where *f*(**q**) is the forward kinematic function generated using RBDL (Felis, 2011). In models with projection, the markers local coordinates, but that along the longitudinal axis of the arm, were set at 0. At each iteration of the nonlinear optimization, observed markers were projected onto the arm longitudinal axis:

$$\mathbf{M}_{obs}^{L} = \mathbf{T}_{G}^{L}(\mathbf{q})\, \mathbf{M}_{obs}^{G} \tag{2a}$$

$$\mathbf{P}_{obs}^{L} = \left[0 \;\; \mathbf{M}_{obs(y)}^{L} \; 0 \; 1\right]^{\mathrm{T}} \tag{2b}$$

$$\mathbf{P}_{obs}^{G} = \mathbf{T}_{L}^{G}(\mathbf{q})\, \mathbf{P}_{obs}^{L}. \tag{2c}$$

where $\mathbf{T}_{G}^{L}$ are 4x4 homogenous transformation matrices from the Global (G) to the Local (L) frames. For each frame, Eq. [1] was solved using a Levenberg-Marquardt algorithm. The initial guess was the generalized coordinates vector found in the previous frame (**q**=**0** in the first frame). At each iteration, the Jacobian matrix of the projection was analytically calculated. The *Arm*, *UpLimb* and *UpLimbP* models were reconstructed using two different marker sets, namely: four markers on each cuff, four skin markers on the arm and forearm, as shown in **Fig. 2**. The *UpLimbS* model was reconstructed with skin markers only.

2.3. Data processing

The variety of movements did not allow to have an angle sequence without passing through gimbal lock positions which makes difficult to reliably maintain continuity in angle time histories (Cutti et al., 2008; Phadke et al., 2011; Senk and Chèze, 2006). To avoid such numerical issues,

the data were post-processed and analyzed as follow. For each model, the scapulohumeral matrices of rotation were calculated using the generalized coordinates. Since high frequency noise may come from multibody kinematic optimization (Fohanno et al., 2014), a zero-lag 2nd order Butterworth filter (cuff-off 5 Hz) was applied to the time histories of each matrix component, which are continuous. Then, in each frame, the nearest orthonormal matrix (**R**) was obtained using Horn's algorithm (Horn et al., 1988):

$$\mathbf{R} = \mathbf{Q}(\mathbf{Q}^{\mathbf{T}}\mathbf{Q})^{-1/2}, \tag{3a}$$

with

$$(\mathbf{Q}^{\mathrm{T}}\mathbf{Q})^{-1/2} = \sum_{i=1}^{3} \frac{1}{\sqrt{\lambda_i}} e_i e_i^{\mathrm{T}}, \tag{3b}$$

where **Q** is the non-orthonormal matrix after signal processing, λ_i the eigen values and e_i the eigen vectors of $\mathbf{Q}^{\mathrm{T}}\mathbf{Q}$.

The scapulohumeral matrix of the *Arm*, *UpLimb* and *UpLimbP* models were compared to that of the *Humerus* model. The misorientation was characterized by four angular deviations, namely: the total deviation value (Eq. [4a], Δ_{tot}) (Begon et al., 2015; de Vries et al., 2010) and the three axial deviations (Eq. [4b-d]), *i.e.* the smallest angles between the vectors *x*, *y* and *z* (de Vries et al., 2010) of the *Arm*, *UpLimb*, *UpLimbP* or *UpLimbS* local frame relative to the local axes of the *Humerus* model:

$$\Delta_{tot}^{m} = \cos^{-1}\left(\frac{\mathrm{trace}\left(\mathbf{R}_{\mathbf{1}}^{\mathbf{T}}\mathbf{R}_{\mathbf{m}}\right) - 1}{2}\right) \tag{4a}$$

$$\Delta_{ant}^{m} = \cos^{-1}(x_1 \cdot x_m) \tag{4b}$$

$$\Delta_{long}^{m} = \cos^{-1}(y_1 \cdot y_m) \tag{4c}$$

$$\Delta_{lat}^{m} = \cos^{-1}(z_1 \cdot z_m) \tag{4d}$$

where the 1-index is relative to the *Humerus* model and *m*-index is relative to the *Arm*, *UpLimb*, *UpLimbP* or *UpLimbS* model. These four angles vary between 0 and 180° and are continuous throughout any movement (*i.e.* without $\pm 2\pi$ jumps) by contrast to Euler/Cardan angles.

To not artificially underestimate the average misorientation, the static phases at the beginning and end of each movement were removed. Since the number of repetitions was different between subjects – due to discomfort or reduced anesthetic time –, trials of similar movements were concatenated before statistical analysis (**Tab. 1**). Then, data were reduced to both average and peak values (noted $\overline{\Delta}$ and $\hat{\Delta}$, respectively) of the total and the axial deviations for each movement and each subject. Results were reported as mean ± standard deviation. Since all the models have a common root, these deviations corresponded to the humeral misorientation. To test the effect of the model, mean and peak deviations were analyzed using separated repeated measures ANOVAs with Bonferroni-corrected contrasts (α=0.05). Based on our hypotheses, the post-hoc tests were limited to *Arm* vs. *UpLimb*, *UpLimb* vs. *UpLimbP* and *UpLimb* vs. *UpLimbS* (α=0.05/3). The gain in accuracy when using a multibody kinematic model and then marker projection was calculated. Finally, 2D correlation coefficients were calculated for time histories of the scapulohumeral unit vectors (lateral, anterior and longitudinal vectors, i.e. the columns of the scapulohumeral rotation matrix) between *Arm*, *UpLimb*, *UpLimbP* or *UpLimbS* models and the *Humerus* model to assess their shape agreement.

3. Results

The last columns of **Tab. 1** summarize the number of frames available in each movement (*i.e.* a series of trials) for calculating average and peak values of humeral deviations. The movements had between 2103±810 and 11269±7325 frames, *i.e.* they last up to 38 seconds. The deviation values that characterized the misorientation in humeral kinematics with respect to the true bone kinematics are summarized in **Tab. 2** and illustrated in **Fig. S1-S4**. When using the *Arm* model (*i.e.* single-body optimization), the average total deviation $\overline{\Delta}_{tot}$ exceeded 10° with peaks up to 21.1°. When using cuff markers, the deviation of the longitudinal axis (Δ_{long}) showed lower values than anterior and lateral deviations. With skin markers, the three axes deviations gave similar values.

All the ANOVAs with the models as independent variables were significant (all $p<10^{-4}$). Post-hoc tests revealed that there was a systematic gain in accuracy (all $p<10^{-4}$) from *Arm* to *UpLimb* models, with both cuff and skin markers. The gain ranged between 37% ($\overline{\Delta}_{lat}$ with skin markers) and 63% ($\hat{\Delta}_{long}$ with skin markers). Using a multibody model, the total deviation dropped on average to 6.1±3.2° and 5.3±1.9° for the cuff and skin markers, respectively, with peaks up to 11.1±4.8° for cuff markers but ≤10° when using skin markers.

With marker projection on the longitudinal arm axis, the gain relative to a standard multibody kinematic optimization (*UpLimb*) was different depending on the set of markers (skin vs. cuff) and the model (*UpLimbP* vs. *UpLimbS*). When markers were stuck on cuffs, average deviations were significantly reduced ($0.0011<p<0.0023$) except for $\hat{\Delta}_{long}$ ($p=0.3219$). The gain on the total deviation was 18%. However, the peak values were not significantly different between *UpLimbP* and *UpLimb* models (all $p>0.6590$). Similar results were found when three skin markers of the arm (all but the medial epicondyle) were projected (*UpLimbS*): average misorientations were

improved up to 20% and the peak values were not improved. Using this innovative projection algorithm (*UpLimbP* with cuff markers and *UpLimbS*), the average error in humeral orientation remained below 5°.

When all the skin markers of the arm were projected (*UpLimbP*) onto its longitudinal axis, results were opposite. The average misorientation was not significantly improved (all $p>0.4843$) and all misorientation peak values were significantly increased (all $p<0.0005$), of about 30%, *i.e.* 3°.

All 2D-correlation coefficients (Table 3) were excellent (r>0.96). They corroborated the results of the ANOVAs since their value increased when using standard multibody kinematic optimization (*UpLimb* vs *Arm*) and even more with projection of cuff markers (*UpLimbP*) and selection of skin markers (*UpLimbS*).

Please insert Tab. 2 here

Please insert Tab. 3 here

4. Discussion

An innovative multibody kinematic optimization algorithm with marker projection was developed, validated against true bone kinematics and compared to single-body and multibody optimizations. Its originality relies on the projection of markers onto a chosen anatomical axis to cancel their deleterious effect on the associated rotation due to large STA. Said algorithm was applied to the upper-limb with projection of the arm markers onto the longitudinal axis. The main findings were that multibody optimization improved the accuracy of 40 to 50% and the projection added an extra 20% when applied to cuff markers or a selection of skin markers. While only four subjects were involved, the findings relied on 4 categories of movements (analytic, ADL, sports activities and range of motion) including 18 movements from 5 to 36 seconds composed of up to 10 trials.

4.1. Accurate humeral kinematics due to multibody optimization

Without multibody optimization, the maximal total deviation exceeded 20° with larger deviation for axial rotation than flexion and abduction (**Fig. S2**). These results agree with study of Hamming et al. (2012), also based on pin data. Large deviations were also found in ADL, sports activities, and range of motion, which reinforces the need of improved models for any kind of motion analysis.

When forearm markers were involved in the multibody system optimization, the deviation dropped to a few degrees with improved 2D correlation coefficients. This confirms the advantage of multibody over single-body optimization on the upper-limb, mainly highlighted using simulation (Roux et al., 2002). The values of the axis deviations $(\Delta_{lat}, \Delta_{ant}, \Delta_{long})$ being similar, the remaining deviation was not associated anymore to the axial rotation. Similar results were found in Lin and Karduna (2013) for three movements exciting one DoF at a time. The present

study generalises the fact that reconstructions including markers on the forearm are efficient to estimate humeral kinematics, based on true bone kinematics and a large variety of movements.

The projection of markers onto a desired axis related to a degree-of-freedom is the most innovative feature in this study. In some conditions, it contributed to improve the accuracy to 5°. The remaining deviation may be associated to the estimation of both the elbow flexion axis and the shoulder joint center locations. Similarly to Lin and Karduna (2013), a functional elbow axis was preferred to the midpoint between the medial and lateral epicondyles. The axis obtained from skin/cuff markers did, however, not coincide with the axis given by the pin markers. Also, the scapulohumeral joint location was not chosen as a gold standard position, often unknown in clinical evaluation. An error of about 5 mm in the scapulohumeral joint location (Michaud et al., 2016) may result in about 5° as shown for the lower-limb (Stagni et al., 2000). As a perspective, the sensitivity of the method to anatomical axis estimation should be tested. By respecting all the recommendations to accurately define a multibody kinematic model and reconstruct the shoulder kinematics, 5° may be the floor value when using non-invasive approaches based on optoelectronic systems.

4.2. Algorithm advantages and limitations

The multibody optimization with selected marker projection improved the joint kinematics for a broad range of movements, for four subjects with different anthropometry (IMC from 21 to 35 kg/m^2). The main advantage of the method is to not have subject- or movement-specific correction, contrary to weighted single-body optimization (Begon et al., 2015) to compensate for the STA of each marker (Blache et al., 2016). However, the selection of markers to be projected remains.

ADL are generally performed with some elbow flexion (Buckley et al., 1996) but most of the biomechanical evaluation in clinics are composed of arm elevation with extended elbow (Robert-Lachaine et al., 2015). Previous algorithms have to be adjusted when the elbow is extended (Cutti et al., 2006; Schmidt et al., 1999). On the other hand, multibody optimization with or without marker projection is robust to movements where the elbow is extended, such as abduction, flexion (ADL category) and arm elevation with neutral or maximal internal/external arm rotation (RoM category).

The effect of marker projection was favorable when using cuff markers or with a selection of skin markers. Indeed, the forearm skin markers were put close to the ulna to minimize the effect of the pro-supination which was not included in the model. However, markers put on the cuff may undergo pro-supination. Similarly to the arm markers, these markers may be projected onto the pro-supination axis of the forearm which should be functionally estimated, as previously suggested by Cutti et al. (2006), since it is not orthonormal to the elbow flexion axis. Further studies are required to assess the algorithm combined with an upper-limb model including pro-supination and hand which may interfere with other DoFs.

This algorithm with marker projection may be applied to other segments, especially the thigh and the scapula to offset the deleterious effect of markers with respect to selected DoFs. Since the thigh has a larger diameter and knee flexion varies between 0 and 20° during the stance phase (Cheze, 2000; Reinschmidt et al., 1997), the projection of the thigh markers onto its longitudinal axis may result in some correction of the thigh rotation. The main limitation would be the estimation of the knee model, which is key in the lower-limb kinematics estimation (Duprey et al., 2010). Regarding the scapula, markers are subject to large STA, except for the acromion and lateral part of the scapula spine (Blache et al., 2016; Matsui et al., 2006). The projection of the

former markers may improve the estimation of the tilt and upward rotation without compromising that of the external rotation. While this algorithm is specific to optoelectronic systems, it could be adapted to electromagnetic/inertial sensors. In fact, the angle associated to the arm rotation should not be introduced into the fusion algorithm (*e.g.* extended Kalman filter) of the upper-limb multibody system.

As in the study of Hamming et al. (2012), the scapulohumeral joint kinematics for all the models was obtained using a common root segment. The error was consequently relative to the humerus only; additional misorientation may come from the scapula. Also, the scapulohumeral joint was modelled as a ball-and-socket joint, while this joint is subject to translations up to 12.4 mm (Dal Maso et al., 2015; Dal Maso et al., 2014). Another drawback of our method was to *a priori* select four skin markers from the seven available in the experiment. This choice was motivated by three reasons. First, the four markers were selected for comparison to the cuff markers (n=4) and, more broadly, to conditions in clinics. Second, the marker put under the deltoid insertion was close to the pin. This marker has shown small STA (Blache et al., 2016) which may be underestimated due to the closeness of the pin. Unlike recommendations of Kontaxis et al. (2009), lateral and medial epicondyles were used because several clinical studies (Anglin and Wyss, 2000) include these markers and our recent study showed a small deformation energy associated to the medial epicondyle (Blache et al., 2016). Finally, the study emphasis was on the multibody kinematic optimisation; further studies should focus on optimal marker sets.

5. Conclusion

To cancel the deleterious effect of some markers on a selected-DoF kinematic reconstruction, an innovative multibody kinematic optimization algorithm with marker projection was presented, where some markers were projected onto the axis associated to the desired DoFs. This innovative

projection algorithm performed better than multibody and single-body optimizations, especially when using markers put on a cuff. Error of humeral orientation was reduced by half to finally be less than 5°.

Conflict of interest statement

Authors declare no conflict of interest.

Acknowledgments

Funding for this project was provided by the NSERC Discovery grant (RGPIN-2014-03912). We would like to acknowledge Raphaël for his contribution to the development of the algorithm and the respect of the guidelines of Lundberg et al. (2014).

References

Anglin, C., Wyss, U.P., 2000. Review of arm motion analyses. Proceedings of the Institution of Mechanical Engineers, Part H: Journal of Engineering in Medicine 214, 541-555.

Begon, M., Dal Maso, F., Arndt, A., Monnet, T., 2015. Can optimal marker weightings improve thoracohumeral kinematics accuracy? Journal of Biomechanics, In Press, Corrected Proof

Begon, M., Wieber, P.B., Yeadon, M.R., 2008. Kinematics estimation of straddled movements on high bar from a limited number of skin markers using a chain model. Journal of Biomechanics 41, 581-586.

Blache, Y., Dumas, R., Lundberg, A., Begon, M., 2016. Main component of soft tissue artefact of the upper-limbs with respect to different arm movements. Journal of Biomechanics (in revision).

Buckley, M.A., Yardley, A., Johnson, G.R., Cams, D.A., 1996. Dynamics of the Upper Limb during Performance of the Tasks of Everyday Living - A Review of the Current Knowledge Base. Journal of Engineering in Medicine 210, 241-247.

Challis, J.H., 1995. A procedure for determining rigid body transformation parameters. Journal of Biomechanics 28, 733-736.

Cheze, L., 2000. Comparison of different calculations of three-dimensional joint kinematics from video-based system data. Journal of Biomechanics 33, 1695-1699.

Cutti, A.G., Cappello, A., Davalli, A., 2005a. A new technique for compensatinf the soft tissue artefact at the upper-arm: in vitro validation. Journal of Mechanics in Medicine and Biology 5, 1-15.

Cutti, A.G., Cappello, A., Davalli, A., 2006. In vivo validation of a new technique that compensates for soft tissue artefact in the upper-arm: Preliminary results. Clinical Biomechanics 21, S13–S19.

Cutti, A.G., Giovanardi, A., Rocchi, L., Davalli, A., Sacchetti, R., 2008. Ambulatory measurement of shoulder and elbow kinematics through inertial and magnetic sensors. Medical & Biological Engineering & Computing 46, 169-178.

Cutti, A.G., Paolini, G., Troncossi, M., Cappello, A., Davalli, A., 2005b. Soft tissue artefact assessment in humeral axial rotation. Gait & Posture 21, 341-349.

Dal Maso, F., Raison, M., Lundberg, A., Arndt, A., Allard, P., Begon, M., 2015. Glenohumeral translations during range-of-motion movements, activities of daily living, and sports activities in healthy participants. Clinical Biomechanics 30, 1002-1007.

Dal Maso, F., Raison, M., Lundberg, A., Arndt, A., Begon, M., 2014. Coupling between 3D displacements and rotations at the glenohumeral joint during dynamic tasks in healthy participants. Clinical Biomechanics 29, 1048-1055.

de Vries, W.H.K., Veeger, H.E.J., Cutti, A.G., Baten, C., van der Helm, F.C.T., 2010. Functionally interpretable local coordinate systems for the upper extremity using inertial & magnetic measurement systems. Journal of Biomechanics 43, 1983-1988.

Dumas, R., Camomilla, V., Bonci, T., Cheze, L., Cappozzo, A., 2014. Generalized mathematical representation of the soft tissue artefact. J Biomech 47, 476-481.

Duprey, S., Cheze, L., Dumas, R., 2010. Influence of joint constraints on lower limb kinematics estimation from skin markers using global optimization. Journal of Biomechanics 43, 2858-2862.

Ehrig, R.M., Taylor, W.R., Duda, G.N., Heller, M.O., 2006. A survey of formal methods for determining the centre of rotation of ball joints. Journal of Biomechanics 39, 2798–2809.

El Habachi, A., Duprey, S., Cheze, L., Dumas, R., 2013. Global sensitivity analysis of the kinematics obtained with a multi-body optimisation using a parallel mechanism of the shoulder. Comput Method Biomec 16, 61-62.

Felis, M.L., 2011. RBDL – Rigid Body Dynamics Library : http://rbdl.bitbucket.org/.

Fohanno, V., Begon, M., Lacouture, P., Colloud, F., 2014. Estimating joint kinematics of a whole body chain model with closed-loop constraints. Multibody System Dynamics 31, 433-449.

Haering, D., Raison, M., Begon, M., 2014. Measurement and description of three-dimensional shoulder range of motion with degrees of freedom interactions. Journal of biomechanical engineering 136, 084502.

Hamming, D., Braman, J.P., Phadke, V., LaPrade, R.F., Ludewig, P.M., 2012. The accuracy of measuring glenohumeral motion with a surface humeral cuff. Journal of Biomechanics 45, 1161-1168.

Horn, B.K.P., Hilden, H.M., Negahdaripour, S., 1988. Closed-form solution of absolute orientation using orthonormal matrices. Journal of the Optical Society of America A 5, 1127-1135.

Jackson, M., Benkhemis, I., Begon, M., Sardain, P., Vallée, C., Lacouture, P., 2012. Identifying the criterion spontaneously minimized during the take-off phase of a sub-maximal long jump through optimal synthesis. Multibody System Dynamics 28, 225-237.

Kontaxis, A., Cutti, A.G., Johnson, G.R., Veeger, H.E.J., 2009. A framework for the definition of standardized protocols for measuring upper-extremity kinematics. Clinical Biomechanics 24, 246-253.

Laitenberger, M., Raison, M., Perie, D., Begon, M., 2015. Refinement of the upper limb joint kinematics and dynamics using a subject-specific closed-loop forearm model. Multibody System Dynamics 33, 413-438.

Lawrence, R.L., Braman, J.P., Staker, J.L., LaPrade, R.F., Ludewig, P.M., 2014. Comparison of 3-dimensional shoulder complex kinematics in individuals with and without shoulder pain, part 2: glenohumeral joint. journal of orthopaedic & sports physical therapy 44, 646-B643.

Lin, Y.-L., Karduna, A.R., 2013. Sensors on the Humerus Are Not Necessary for an Accurate Assessment of Humeral Kinematics in Constrained Movements. Journal of Applied Biomechanics 29, 496-500.

Ludewig, P.A., Cook, T.M., Shields, R.K., 2002. Comparison of surface sensor and bone-fixed measurement of humeral motion. Journal of Applied Biomechanics 18, 163-170.

Lundberg, A., Aguilera, A., Cappozzo, A., Arndt, A., Begon, M., 2014. Entropy in the List of Authors of Scientific Papers. Annals of improbable research 20, 15-17.

Matsui, K., Shimada, K., Andrew, P.D., 2006. Deviation of skin marker from bone target during movement of the scapula. Journal of Orthopaedic Science 11, 180-184.

Michaud, B., Jackson, M., Arndt, A., Lundberg, A., Begon, M., 2016. Determining in vivo sternoclavicular, acromioclavicular and glenohumeral joint centre locations from skin markers, CT-scans and intracortical pins: A comparison study. Medical engineering & physics 38, 290-296.

Monnet, T., Begon, M., Vallée, C., Lacouture, P., 2010. Improvement of the input data in biomechanics: kinematic and body segment inertial parameters, in: Jerrod H. Levy (Ed.), Biomechanics: Principles, Trends and Applications. Nova Science Publishers, Inc., pp. 353-385.

O'Brien, J.F., Bodenheimer Jr, R.E., Brostow, G.J., Hodgins, J.K., 1999. Automatic joint parameter estimation from magnetic motion capture data. Georgia Institute of Technology.

Phadke, V., Braman, J.P., LaPrade, R.F., Ludewig, P.M., 2011. Comparison of glenohumeral motion using different rotation sequences. Journal of Biomechanics 44, 700-705.

Rab, G., Petuskey, K., Bagley, A., 2002. A method for determination of upper extremity kinematics. Gait & Posture 15, 113-119.

Reinschmidt, C., van den Bogert, A.J., Lundberg, A., Nigg, B.M., Murphy, N., Stacoff, A., Stano, A., 1997. Tibiofemoral and tibiocalcaneal motion during walking: external vs. skeletal markers. Gait & Posture 6, 98-109.

Robert-Lachaine, X., Allard, P., Gobout, V., Begon, M., 2015. Shoulder Coordination During Full-Can and Empty-Can Rehabilitation Exercises. Journal of Athletic Training 50, 1117-1125.

Roux, E., Bouilland, S., Godillon-Maquinghen, A.P., Bouttens, D., 2002. Evaluation of the global optimisation method within the upper limb kinematics analysis. Journal of Biomechanics 35, 1279-1283.

Schmidt, R., Disselhorst-Klug, C., Silny, J., Rau, G., 1999. A marker-based measurement procedure for unconstrained wrist and elbow motions. Journal of Biomechanics 32, 615-621.

Senk, M., Chèze, L., 2006. Rotation sequence as an important factor in shoulder kinematics. Clinical Biomechanics 21, S3-S8.

Stagni, R., Leardini, A., Cappozzo, A., Grazia Benedetti, M., Cappello, A., 2000. Effects of hip joint centre mislocation on gait analysis results. Journal of Biomechanics 33, 1479-1487.

van Andel, C.J., Wolterbeek, N., Doorenbosch, C.A., Veeger, D.H., Harlaar, J., 2008. Complete 3D kinematics of upper extremity functional tasks. Gait & Posture 27, 120-127.

Wu, G., van der Helm, F.C.T., Veeger, H.E.J., Makhsous, M., Van Roy, P., Anglin, C., Nagels, J., Karduna, A.R., McQuade, K., Wang, X.G., Werner, F.W., Buchholz, B., 2005. ISB recommendation on definitions of joint coordinate systems of various joints for the reporting of human joint motion - Part II: shoulder, elbow, wrist and hand. Journal of Biomechanics 38, 981-992.

Figures and Tables

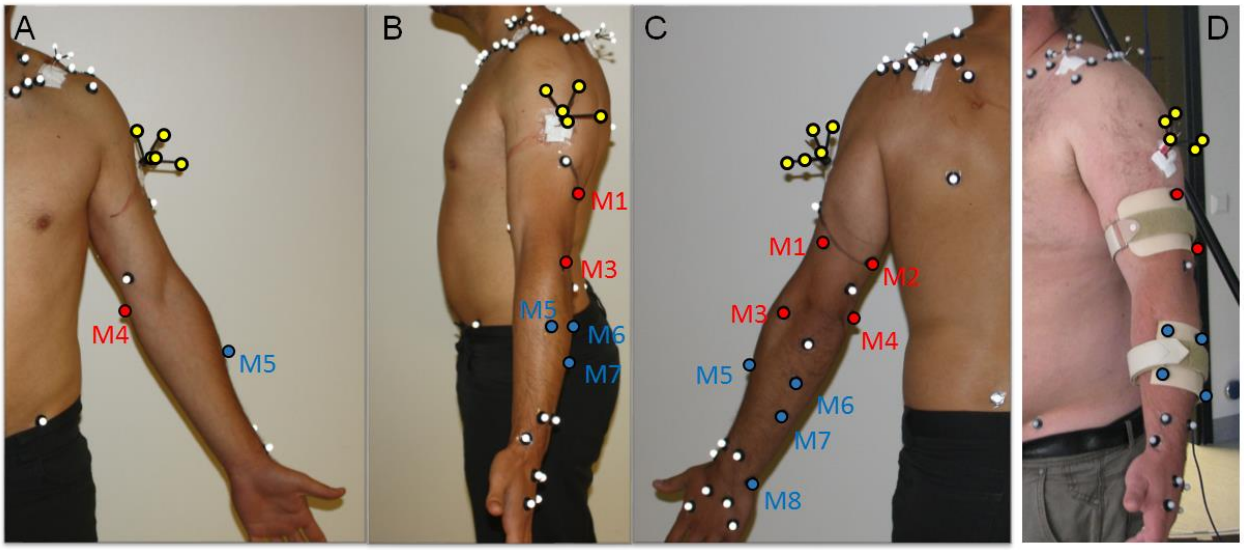

Fig. 1: (A-C) Markers were put on an intracortical pin (in yellow), on the skin of the arm (red) and forearm (blue) and (D) on the cuffs. Specifically, the skin markers were placed as follow: laterally (M1) and medially (M2) to the belly of the triceps, lateral epicondyle (M3), medial epicondyle (M4), medial (M5) and lateral (M6) aspects of the brachioradialis, at the end of the triangle formed by the brachioradialis (M7) and on the ulnar styloid (M8).

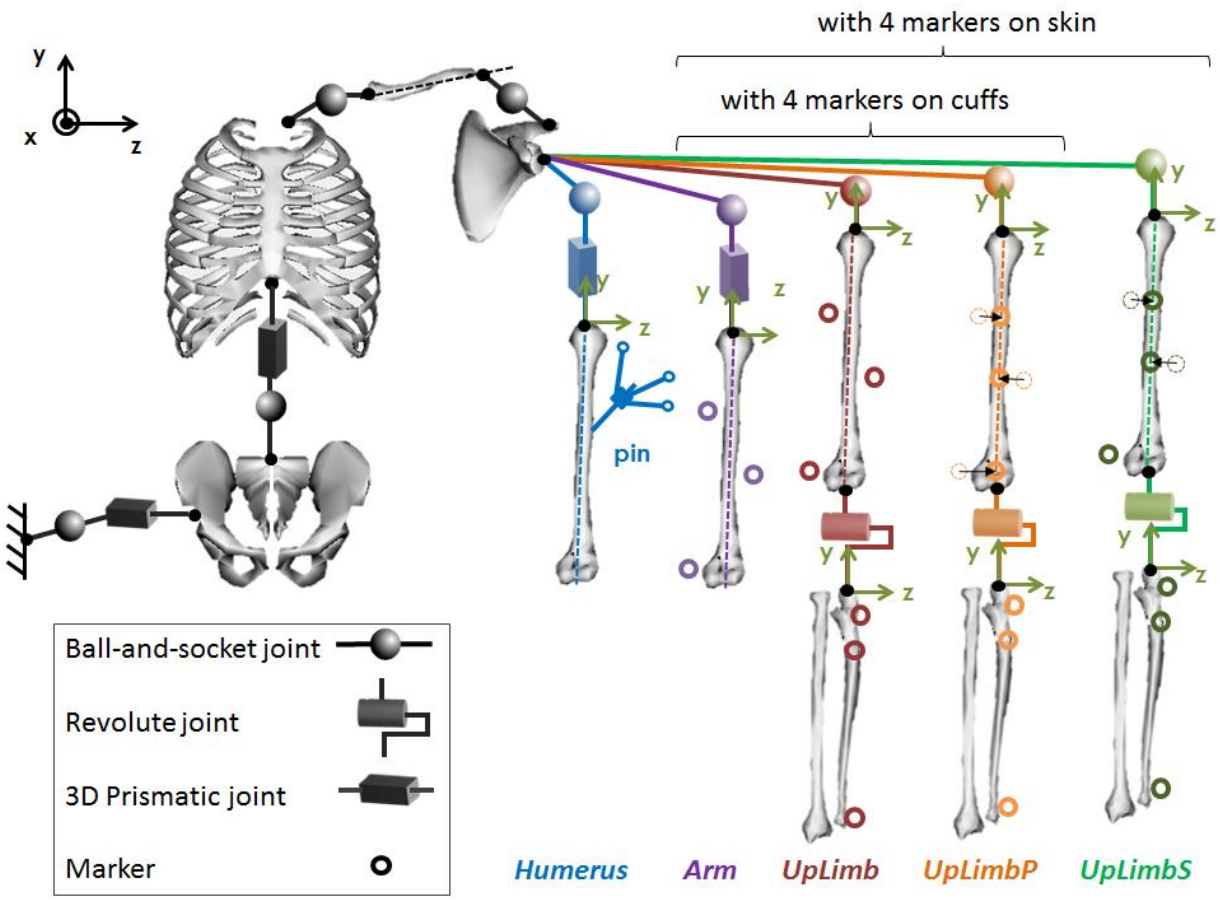

Fig. 2: Five models with the common root (pelvis-thorax-clavicle-scapula) and their degrees-of-freedom, from left to right: *Humerus* with 6 DoFs and based on the markers attached to the intracortical pin screw in the humerus; *Arm* with 6 DoFs and based on the skin or cuff markers; *UpLimb* with 3 DoFs at the scapulohumeral joint and 1 DoF at the elbow based on skin and cuff markers; *UpLimbP* similar to *UpLimb* but all markers on the arm (skin or cuff) are projected onto the longitudinal axis; *UpLimbS* similar to *UpLimb* but three markers on the arm (M1-3, not M4) are projected onto the longitudinal axis.

Tab. 1: Description of the four categories of movements. The last two columns indicate the number of frames retained (mean±SD) for the analysis using trials with markers put on the skin or fixed on the cuffs (sampling rate: 300 Hz).

Categories	Movements	Comments	Number of Frames	
			Skin	Cuff
Analytic movements	1. Abduction	up to 10 repetitions	11188±6548	9067±6158
	2. Flexion	up to 10 repetitions	11269±7325	9550±6240
	3. Internal-External rotations with adducted arm		3806±1750	4042±1165
	4. Internal-External rotations with 90° of arm elevation in the scapular plan		2782±1572	3464±582
Activities of daily living (mimics of)	5. Eat**	with a spoon but no food	2988±866	2449±603
	6. Comb	with a comb	4607±1437	3851±1251
	7. Attach a bra in the back**	reach back	3394±989	3089±1321
	8. Wash armpit*,**	reach opposite armpit	1987±870	2103±810
	9. Reach front and back pockets	ipsolateral pocket	5979±3358	4899±2782
Sports activities (mimics of)	10. Tennis forehands and backhands	with a racket but no ball	4355±1042	N/A
	11. Throw a ball	without ball	3243±1139	N/A
	12. Clap		1547±520	N/A
	13. Punch*	in a piece of foam*	3088±988	N/A
	14. Hockey shoot	with a stick but no puck	3962±130	N/A
Movements with maximal range of motion	15. Maximal arm elevation with the arm maximally internally rotated	in adduction, flexion, abduction and extension	4823±1757	N/A
	16. Maximal arm elevation with the arm maximally externally rotated	in adduction, flexion, abduction and extension	5511±1058	N/A
	17. Maximal arm elevation with the arm in neutral rotation	in adduction, flexion, abduction and extension	4110±1516	N/A
	18. Maximal internal-external rotation	for each combination of adduction, flexion, abduction and extension at 0°, 45°, 90°, 135° and 180°	9833±3827	N/A

* This movement was not performed by subject 1 with skin markers.
** This movement was not performed by subject 3 with cuffs.
N/A not applicable: this movement was not performed with cuff.

Tab. 2: Mean and standard deviation (SD) in degrees (°) of the four deviations (average $\overline{\Delta}$ and peak $\hat{\Delta}$ values) for models *Arm*, *UpLimb*, *UpLimbP* and *UpLimbS* relative to Humerus. P-values of the ANOVA and post-hoc tests are in bold when significant and the gain in accuracy (*UpLimb* vs *Arm*, *UpLimbP* vs *UpLimb* and *UpLimbS* vs *UpLimb*) is provided. Values are summarized for two marker sets, namely A) four cuff markers, B) four skin markers on the arm and forearm.

A) Cuff markers (n=35, 9 movements x 4 participants, except for subject 3 who performed 8 movements)

	Arm		*UpLimb*			*UpLimbP*			*p*-values		
	Mean	(SD)	Mean	(SD)	Gain	Mean	(SD)	Gain	ANOVA	*UpLimb* vs *Arm*	*UpLimb* vs *UpLimbP*
$\overline{\Delta}_{tot}$	10.5	(5.4)	6.1	(3.2)	**42%**	5.0	(2.3)	**18%**	**0.0000**	**0.0000**	**0.0023**
$\overline{\Delta}_{lat}$	9.4	(5.4)	5.4	(3.2)	**42%**	4.2	(2.1)	**22%**	**0.0000**	**0.0000**	**0.0017**
$\overline{\Delta}_{ant}$	9.4	(5.0)	5.3	(2.7)	**43%**	4.1	(2.0)	**22%**	**0.0000**	**0.0000**	**0.0011**
$\overline{\Delta}_{long}$	5.5	(3.3)	3.5	(2.4)	**36%**	3.3	(2.0)	5%	**0.0000**	**0.0000**	0.3219
$\hat{\Delta}_{tot}$	19.1	(8.7)	11.1	(4.8)	**42%**	10.9	(5.2)	2%	**0.0000**	**0.0000**	0.8067
$\hat{\Delta}_{lat}$	17.8	(8.2)	9.9	(4.6)	**44%**	9.7	(4.6)	3%	**0.0000**	**0.0000**	0.7112
$\hat{\Delta}_{ant}$	17.2	(7.8)	10.2	(4.6)	**41%**	9.9	(5.1)	3%	**0.0000**	**0.0000**	0.6590
$\hat{\Delta}_{long}$	12.1	(6.0)	7.4	(4.3)	**39%**	7.5	(4.2)	-2%	**0.0000**	**0.0000**	0.6970

B) Skin markers (n=70, 18 movements x 4 participants, except for subject 1 who performed 16 movements)

	Arm		*UpLimb*			*UpLimbP*			*UpLimbS*			*p*-values			
	Mean	(SD)	Mean	(SD)	Gain	Mean	(SD)	Gain	Mean	(SD)	Gain	ANOVA	*UpLimb* vs *Arm*	*UpLimbP* vs *UpLimb*	*UpLimbS* vs *UpLimb*
$\overline{\Delta}_{tot}$	10.2	(5.3)	5.3	(1.9)	**48%**	5.3	(1.8)	0%	4.4	(1.5)	**16%**	**0.0000**	**0.0000**	0.9835	**0.0020**
$\overline{\Delta}_{lat}$	6.8	(4.0)	4.3	(1.7)	**37%**	4.1	(1.7)	4%	3.4	(1.4)	**20%**	**0.0000**	**0.0000**	0.4843	**0.0010**
$\overline{\Delta}_{ant}$	8.4	(4.5)	4.7	(1.8)	**44%**	4.7	(1.7)	-1%	3.9	(1.4)	**17%**	**0.0000**	**0.0000**	0.9144	**0.0023**
$\overline{\Delta}_{long}$	8.7	(4.8)	3.6	(1.5)	**59%**	3.6	(1.3)	-1%	3.0	(1.1)	**14%**	**0.0000**	**0.0000**	0.8370	**0.0017**
$\hat{\Delta}_{tot}$	21.1	(12.2)	9.6	(3.9)	**54%**	12.4	(4.9)	**-29%**	9.3	(3.7)	4%	**0.0000**	**0.0000**	**0.0000**	0.5362
$\hat{\Delta}_{lat}$	17.0	(10.5)	8.5	(3.2)	**50%**	11.2	(4.7)	**-32%**	8.2	(3.6)	3%	**0.0000**	**0.0000**	**0.0000**	0.6368
$\hat{\Delta}_{ant}$	17.9	(9.7)	8.9	(3.7)	**50%**	11.6	(4.7)	**-30%**	8.5	(3.4)	5%	**0.0000**	**0.0000**	**0.0001**	0.4757
$\hat{\Delta}_{long}$	18.7	(11.7)	6.8	(3.2)	**63%**	8.5	(3.9)	**-25%**	6.8	(3.0)	1%	**0.0000**	**0.0000**	**0.0005**	0.9295

Tab. 3: Mean and standard deviation (SD) of the 2D correlation coefficients of lateral (r_{lat}), anterior (r_{ant}) and longitudinal (r_{long}) axes of the *Arm*, *UpLimb*, *UpLimbP* and *UpLimbS* models and the *Humerus* model. Values are summarized for two marker sets, namely A) four cuff markers, B) four skin markers on the arm and forearm.

A) Cuff markers (n=35, 9 movements x 4 participants, except for subject 3 who performed 8 movements)

	Arm		*UpLimb*		*UpLimbP*	
	Mean	(SD)	Mean	(SD)	Mean	(SD)
r_{lat}	0.985	(0.016)	0.996	(0.004)	0.997	(0.003)
r_{ant}	0.965	(0.036)	0.988	(0.015)	0.992	(0.014)
r_{long}	0.998	(0.003)	0.999	(0.002)	0.999	(0.002)

B) Skin markers (n=70, 18 movements x 4 participants, except for subject 1 who performed 16 movements)

	Arm		*UpLimb*		*UpLimbP*		*UpLimbS*	
	Mean	(SD)	Mean	(SD)	Mean	(SD)	Mean	(SD)
r_{lat}	0.978	(0.115)	0.998	(0.002)	0.998	(0.002)	0.998	(0.002)
r_{ant}	0.975	(0.074)	0.994	(0.005)	0.994	(0.005)	0.996	(0.005)
r_{long}	0.981	(0.023)	0.998	(0.002)	0.998	(0.002)	0.998	(0.002)